Five-partite entanglement generation in a high-Q microresonator

Yutian Wen,[1] Xufei Wu,[1] Rongyu Li,[1] Qiang Lin,[2] and Guangqiang He[1,*]

[1]*State Key Lab of Advanced Optical Communication Systems and Networks, Department of Electronic Engineering, Shanghai Jiao Tong University, Shanghai 200240, China*

[2]*Department of Electrical and Computer Engineering, University of Rochester, New York 14627, USA*

(Received 22 December 2014; published 9 April 2015)

We propose to produce five-partite entanglement via cascaded four-wave mixing in a high-Q microresonator that may become a key to future one-way quantum computation on chip. A theoretical model is presented for the underlying continuous-variable entanglement among the generated comb modes that is expansible to more complicated scenarios. We analyze the entanglement condition when the van Loock and Furusawa criteria are violated and discuss the device parameters for potential experimental realization that may be utilized to build an integrated compact five-partite entanglement generator. The proposed approach exhibits great potential for future large-scale integrated full optical quantum computation on chip.

DOI: 10.1103/PhysRevA.91.042311 PACS number(s): 03.67.Bg, 42.65.Wi, 03.67.Lx, 42.65.Yj

I. INTRODUCTION

Quantum computation (QC) is expected to provide exponential speedup for particular mathematical problems such as integer factoring [1] and quantum system simulation [2]. However, any practical QC system must overcome the inevitable decoherence problem and achieve scalability. The traditional "circuit" QC model keeps quantum information in a physical system where quantum memory units undergo precise controlled unitary evolution simultaneously, leading to serious scalability issues. To circumvent this challenge, an "one-way" quantum computation model was proposed [3], where quantum information exists virtually in a cluster state [4] and one can perform any desired quantum algorithm by conducting a sequence of local measurements. With this approach, the most challenging part is now transferred from conducting the unitary operation on a large scale to the generation of a cluster state or, more generally, a universal multipartite entangled state. The aim of this paper is to investigate the possibility of a novel integrated approach for generating multipartite entangled states.

Optical frequency combs (OFCs) have been shown to be capable of preserving cluster states [5,6]. An OFC is a light source composed of equally spaced discrete frequency components, as illustrated in Fig. 1(a). Actual OFCs might extend to an extremely broad band with hundreds of frequency components [7,8], each of which corresponds to a comb mode (marked by a mode number; say, m). OFCs are favorable for QC for their robustness against decoherence [6], since photons are less likely to interact with the environment compared with other physical systems such as atoms [5].

OFCs have already been utilized in many applications such as frequency metrology, telecommunications, optical and microwave waveform synthesis, and molecular spectroscopy [7,8]. Conventionally, OFCs are generated in mode-locked lasers that are usually bulky, difficult to operate, and susceptible to environmental perturbations [6]. It was recently reported that OFCs can also be generated from monolithic microresonators [9,10] through cascaded four-wave mixing (FWM).

In a high-Q microresonator with appropriate dispersion, an intense pump wave launched into a cavity mode excites four-wave mixing processes among different cavity modes via the optical Kerr effect [10]. There are dominantly two types of FWM, degenerate and nondegenerate, which are illustrated in Fig. 1(b). Due to momentum conservation among the interacting photons, a degenerate process converts two identical photons in a same mode at m into two dissimilar photons at modes $m-1$ and $m+1$, respectively. Similarly, a nondegenerate process converts two photons from modes m and $m+1$ into two new photons at modes $m-1$ and $m+2$. The iteration of these two processes thus produces an optical frequency comb [10], with a spectral extent determined by the group-velocity dispersion of the device.

The beauty of such a scheme lies in the nature of high-Q microresonators. First, the optical field is strongly confined inside a small volume, leading to significantly enhanced nonlinear optical interactions. Second, due to the exceptionally high quality factors Q of microresonators, the photon lifetime inside the cavity is much longer than that in traditional cavities so that different frequency components have enough time to entangle with each other. Finally, the integrated chip-scale platform of microresonators exhibit great potential for eventually realizing a large-scale integrated full optical quantum computer [11].

These facts inspired us to explore the potential of OFCs for producing multipartite entangled states inside a microresonator. Although two-mode quantum squeezing has been intensively investigated for parametric processes [12–21], the quantum properties of microresonator-based frequency comb generation has not yet been fully addressed. On the other hand, there have been both theoretical analyses of [22–25]and experimental investigations [26–30] into photon-pair generation inside micro- or nanophotonic devices. Yet all of them focused on the bipartite discrete-variable entanglement whose methodology cannot be applied to the analysis of entanglement among three or more frequency components. In this paper, we present a theoretical model to describe the five-partite continuous-variable entanglement among frequency-comb modes. We solve the Fokker–Planck equation in the P representation and analyze the entanglement condition when van Loock and Furusawa criteria are violated.

*gqhe@sjtu.edu.cn

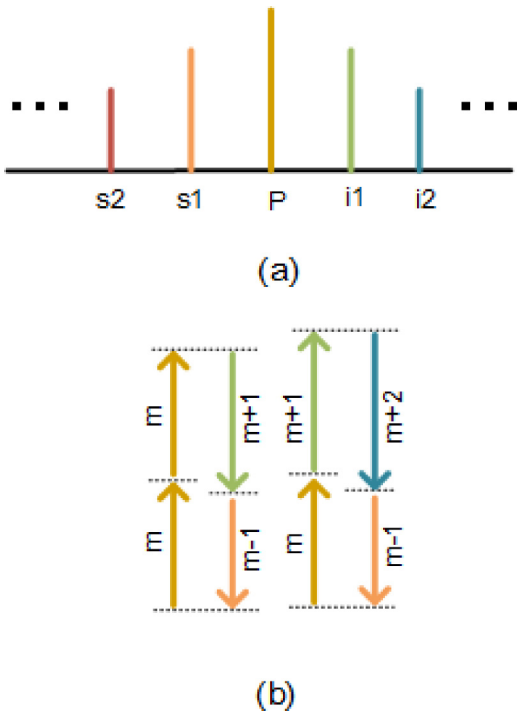

FIG. 1. (Color online) (a) The spectrum of an ideal frequency comb is discrete, equally spaced, and covers a wide band. (b) Energy-level diagram of degenerate (left) and nondegenerate (right) FWM.

The rest of this paper is arranged as follows: in Sec. II, we present a system model to describe the cascade four-wave mixing process in a high-Q microresonator. We then analyze the quantum fluctuations of the cavity fields and the five-partite entanglement in Secs. III–V. We discuss the resulting quantum fluctuations on the cavity output and their dependence on the cavity parameters and operation conditions in Sec. VI. The main conclusions are summarized in Sec. VII.

II. SYSTEM MODEL

We consider a generic scheme of comb generation, as shown in Fig. 2, where a continuous-wave pump wave is launched into a microresonator to excite the FWM process. The resulting frequency comb output from the cavity is then separated into individual frequency components for analysis [31].

In general, the number of comb modes produced is determined by the device dispersion, the pump power, and the cavity detuning [11,32,33]. We consider here a simple

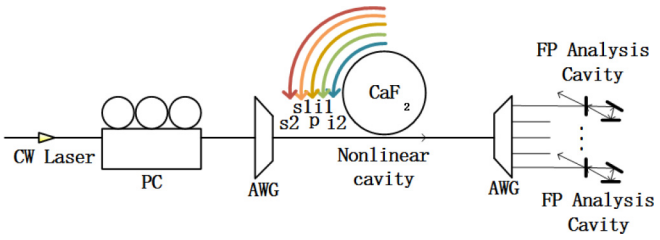

FIG. 2. (Color online) OFC generator with a calcium fluoride cavity and angle-polished fiber couplings. "CW" indicates continuous wave. "PC" indicates polarization controller. "AWG" indicates arrayed waveguide grating.

frequency comb that consists of five modes, as shown in Fig. 1(a). Such a comb number can be achieved by engineering the group-velocity dispersion to limit the phase matching bandwidth of the FWM process.

The FWM process governing the comb generation originates from the optical Kerr effect. With an electric field composed of five frequency components, the interaction Hamiltonian of the Kerr effect is given by [34–36] $V = \hbar(g/2) : (a_p + a_{s1} + a_{i1} + a_{s2} + a_{i2} + \text{H.c.})^4 :$, where ": $\cdots$:" stands for normal ordering and g is the coupling coefficient given as $g = n_2\hbar\omega_0^2 c/(\mathcal{V}n_0^2)$, where n_2 is nonlinear refractive index that characterizes the strength of the optical nonlinearity, n_0 is the linear refractive index of the material, c is the speed of light in vacuum, and $\mathcal{V}$ is the effective mode volume [11,34]. The coupling coefficient is assumed to be independent of frequency, because the frequency difference between neighboring combs is negligible [34]. Consequently, the Hamiltonian for the comb-generation system is found to be

$$H = H_{\text{free}} + H_{\text{pump}} + H_{\text{int}}, \tag{1}$$

$$H_{\text{free}} = \hbar\sum_k \omega_k a_k^\dagger a_k, \quad H_{\text{pump}} = i\hbar\epsilon a_p^\dagger + \text{H.c.}, \tag{2}$$

$$\begin{aligned} H_{\text{int}} = {} & i\frac{g}{2}\hbar\sum_k a_k^\dagger a_k^\dagger a_k a_k + ig\hbar\sum_{k\neq t} a_k^\dagger a_t^\dagger a_t a_k \\ & + ig\hbar\big(a_{s1}^\dagger a_{i1}^\dagger a_p^2 + a_{s2}^\dagger a_{i1}^\dagger a_{s1} a_p + a_{s1}^\dagger a_{i2}^\dagger a_{i1} a_p \\ & + a_{s2}^\dagger a_p^\dagger a_{s1}^2 + a_{i2}^\dagger a_p^\dagger a_{i1}^2\big) + \text{H.c.}, \end{aligned} \tag{3}$$

where $k,t = p,s1,s2,i1,i2$, and ϵ is the pump field that enters the resonator, which is described classically because of its intense amplitude [34].

The interaction Hamiltonian in Eq. (3) consists of three parts responsible for self-phase modulation, cross-phase modulation, and four-wave mixing. It is easy to verify that the first two parts automatically vanish in the P representation [12]. For the cascaded FWM, the pump wave produces the $s1$ and $i1$ modes via degenerate FWM, $2\omega_p \to \omega_{s1} + \omega_{i1}$, which in turn produces $s2$ and $i2$ by hyperparametric oscillation dominantly via the following FWM processes: $2\omega_{s1} \to \omega_p + \omega_{s2}$, $2\omega_{i1} \to \omega_p + \omega_{i2}$, $\omega_{s1} + \omega_p \to \omega_{i1} + \omega_{s2}$, and $\omega_{i1} + \omega_p \to \omega_{s1} + \omega_{i2}$. Compared to these processes, $2\omega_p \to \omega_{s2} + \omega_{i2}$ and $\omega_{s1} + \omega_{i2}$ play minor roles due to larger phase mismatch and the smaller intensities of $s1$ and $i1$ compared to the pump. Although they might help the phase-locking mechanism, they are less dominant compared to others. We thus neglect these two processes in our analysis.

A microresonator is an open system since it not only exhibits intrinsic scattering loss with a photon decay rate of γ_{k0} (for mode k) but also couples waves to the coupling waveguide with an external coupling rate of γ_{kc}. To describe such an open system, we introduce the loss and out-coupling terms as

$$L_k\rho = \gamma_k(2a_k\rho a_k^\dagger - a_k^\dagger a_k\rho - \rho a_k^\dagger a_k), \tag{4}$$

in which ρ is the density matrix of the five modes under consideration. $\gamma_k = \gamma_{k0} + \gamma_{kc}$ stands for the damping rate of the loaded cavity. The output fields are determined by the

well-known input-output relations, which are given as [37]

$$b_{\text{out}} - b_{\text{in}} = \sqrt{\gamma}a, \tag{5}$$

where b is the boson annihilation operator for the bath field outside the cavity.

III. EQUATIONS OF MOTION FOR THE FULL HAMILTONIAN

With the system model developed in Sec. II, we can now obtain the master equation for the five cavity modes as

$$\frac{\partial\rho}{\partial t} = -\frac{i}{\hbar}[H_{\text{pump}} + H_{\text{int}}, \rho] + \sum_{k=1}^{5} L_k\rho. \tag{6}$$

The free Hamiltonian does not show up in Eq. (6) because of the rotating-wave approximation [37] $a_k \to e^{-i\omega_k t}a_k$.

The master equation above can be converted into the equivalent c-number Fockker–Planck equation in P representation, which can be written as a completely equivalent stochastic differential equation as [12]

$$\frac{\partial\boldsymbol{\alpha}}{\partial t} = \mathbf{F} + \mathbf{B}\boldsymbol{\eta}, \tag{7}$$

where $\boldsymbol{\alpha} = [\alpha_p,\alpha_{s1},\alpha_{i1},\alpha_{s2},\alpha_{i2},\alpha_p^*,\alpha_{s1}^*,\alpha_{i1}^*,\alpha_{s2}^*,\alpha_{i2}^*]^T$, and $\boldsymbol{F} = [f, f^*]^T$ is the main part of the system's evolution in which f is given by

$$f = \begin{pmatrix} \epsilon - \gamma_p\alpha_p - 2g\alpha_p^*\alpha_{s1}\alpha_{i1} - g\alpha_{s1}^*\alpha_{s2}\alpha_{i1} - g\alpha_{i1}^*\alpha_{i2}\alpha_{s1} + g\alpha_{s1}^2\alpha_{s2}^* + g\alpha_{i1}^2\alpha_{i2}^* \\ -\gamma_{s1}\alpha_{s1} + g\alpha_p^2\alpha_{i1}^* + g\alpha_{i1}\alpha_p\alpha_{i2}^* - g\alpha_{s2}\alpha_{i1}\alpha_p^* - 2g\alpha_p\alpha_{s2}\alpha_{s1}^* \\ -\gamma_{i1}\alpha_{i1} + g\alpha_p^2\alpha_{s1}^* + g\alpha_{s1}\alpha_p\alpha_{s2}^* - g\alpha_{i2}\alpha_{s1}\alpha_p^* - 2g\alpha_p\alpha_{i2}\alpha_{i1}^* \\ -\gamma_{s2}\alpha_{s2} + g\alpha_{s1}\alpha_p\alpha_{i1}^* + g\alpha_{s1}^2\alpha_p^* \\ -\gamma_{i2}\alpha_{i2} + g\alpha_{i1}\alpha_p\alpha_{s1}^* + g\alpha_{i1}^2\alpha_p^* \end{pmatrix}.$$

Matrix $\mathbf{B}$ contains the coefficients of the noise terms which is obtained through $\mathbf{BB}^T = \mathbf{D}$ in which the diffusion matrix $\mathbf{D}$ is given by

$$\mathbf{D} = \begin{pmatrix} \mathbf{d} & 0 \\ 0 & \mathbf{d}^* \end{pmatrix},$$

where d is a matrix with the form of

$$d = g\begin{pmatrix} -2\alpha_{s1}\alpha_{i1} & -\alpha_{s2}\alpha_{i1} & -\alpha_{s1}\alpha_{i2} & \alpha_{s1}^2 & x\alpha_{i1}^2 \\ -\alpha_{s2}\alpha_{i1} & -2\alpha_p\alpha_{s2} & \alpha_p^2 & 0 & \alpha_{i1}\alpha_p \\ -\alpha_{s1}\alpha_{i2} & \alpha_p^2 & -2\alpha_p\alpha_{i2} & \alpha_{s1}\alpha_p & 0 \\ \alpha_{s1}^2 & 0 & \alpha_{s1}\alpha_p & 0 & 0 \\ \alpha_{i1}^2 & \alpha_{i1}\alpha_p & 0 & 0 & 0 \end{pmatrix}.$$

In Eq. (7), $\boldsymbol{\eta} = [\eta_1(t),\eta_2(t),\eta_3(t),\eta_4(t),\eta_5(t),\text{c.c.}]^T$, where η_i are real noise terms characterized by $\langle\eta_i(t)\rangle = 0$ and $\langle\eta_i(t)\eta_j(t)\rangle = \delta_{ij}\delta(t-t')$.

IV. LINEARIZED QUANTUM-FLUCTUATION ANALYSIS

To solve Eq. (7), we decompose the system variables into their steady-state (classical) values and quantum fluctuations as $\alpha_i = A_i + \delta\alpha_i$. Since the quantum fluctuations are much smaller than the steady-state values, we can thus apply the linearization analysis to find the spectra for the cavity outputs. To simplify the analysis, we assume that the five comb modes exhibit a same photon decay rate and a same external coupling rate ($\gamma_k = \gamma,\gamma_{kc} = \gamma_c,\gamma_{k0} = \gamma_0,k = p,s1,s2,i1,i2$), since their frequencies are not far from each other. Noticing that the symmetry between the signal photons ($s1$ and $s2$) and their idler counterparts ($i1$ and $i2$) because of the conjugate nature of the FWM process, we may use the same variable to denote the c number of a pair, i.e., $A_{i1} = A_{s1} = A_a$ and $A_{i2} = A_{s2} = A_b$.

The steady state of the comb generation can be found by setting $\partial\boldsymbol{\alpha}/\partial t$ in Eq. (7) to zero, which results in a pump threshold of

$$\epsilon_{th} = \gamma\sqrt{\gamma/g}. \tag{8}$$

When $\epsilon < \epsilon_{th}$, the steady-state cavity fields are given by $A_p = \epsilon/\gamma$ and $A_j = 0$ ($i = i1,s1,i2,s2$). When $\epsilon > \epsilon_{th}$, the steady states become

$$A_p = \frac{\varepsilon + \sqrt{\varepsilon^2 + (3\gamma^3)/g}}{3\gamma}, \tag{9}$$

$$A_{i1} = A_{s1} = A_a = \sqrt{\frac{\gamma}{4g}\left(1 - \frac{\gamma}{gA_p^2}\right)}, \tag{10}$$

$$A_{i2} = A_{s2} = A_b = \frac{2gA_pA_a^2}{\gamma}. \tag{11}$$

In the present scheme we only consider the situation for the field modes to oscillate above the threshold. Note that the γ is of the order of $10^5\ \text{s}^{-1}$, $A_p = [\varepsilon + (\varepsilon^2 + 3\varepsilon_{th}^2)^{1/2}]/(3\gamma) < \varepsilon/\gamma$ is actually much smaller than ϵ, so our nondepletion assumption is self-consistent.

With the steady-state solution, we cannot find the equations of motion governing the quantum fluctuations of the comb modes as

$$\frac{\partial}{\partial t}\delta\boldsymbol{\alpha} = \boldsymbol{M}\delta\boldsymbol{\alpha} + \boldsymbol{B}\boldsymbol{\eta}, \tag{12}$$

where $\delta\boldsymbol{\alpha} = [\delta\alpha_p,\delta\alpha_{s1},\delta\alpha_{i1},\delta\alpha_{s2},\delta\alpha_{i2},\text{H.c.}]^T$. $\boldsymbol{M}$ is the drift matrix given by

$$\boldsymbol{M} = \begin{pmatrix} \boldsymbol{m}_1 & \boldsymbol{m}_2 \\ \boldsymbol{m}_2^* & \boldsymbol{m}_1^* \end{pmatrix},$$

$$\boldsymbol{m}_1 = \begin{pmatrix} -\gamma & -G & -G & -gA_a^2 & -gA_a^2 \\ G & -\gamma & 0 & -3gA_pA_a & 0 \\ G & 0 & -\gamma & 0 & -3gA_pA_a \\ gA_a^2 & 3gA_pA_a & 0 & -\gamma & 0 \\ gA_a^2 & 0 & 3gA_pA_a & 0 & -\gamma \end{pmatrix},$$

$$\boldsymbol{m}_2 = g\begin{pmatrix} -2A_a^2 & -A_aA_b & -A_a\alpha_b & A_a^2 & A_a^2 \\ -A_aA_b & -2A_pA_b & A_p^2 & 0 & A_aA_p \\ -A_a\alpha_b & A_p^2 & -2A_pA_b & A_aA_p & 0 \\ A_a^2 & 0 & A_aA_p & 0 & 0 \\ A_a^2 & A_aA_p & 0 & 0 & 0 \end{pmatrix},$$

where

$$G = -gA_aA_b - 2gA_pA_a + 2gA_aA_b.$$

For the linearized quantum-fluctuation analysis to be valid. the fluctuations must remain small compared to the mean values. If the requirement that the real part of the eigenvalues of $-\boldsymbol{M}$ stay non-negative is satisfied, the fluctuation equations will describe an Ornstein–Uhlenbeck process [38] for which the intracavity spectral correlation matrix is

$$\boldsymbol{S}(\omega) = (-\boldsymbol{M} + i\omega\boldsymbol{I})^{-1}\,\boldsymbol{D}(-\boldsymbol{M}^T - i\omega\boldsymbol{I})^{-1}. \tag{13}$$

All the correlations required to study the measurable extracavity spectra are contained in this intracavity spectral matrix. We have checked the stability numerically for the rest of discussion.

In order to investigate the multipartite entanglement, we define quadrature operators for each mode as

$$X_k = a_k + a_k^\dagger, \quad Y_k = -i(a_k - a_k^\dagger), \tag{14}$$

with a commutation relationship of $[X_k,Y_k] = 2i$. Based on such definition, $V(X_k) \leqslant 1$ will indicate a squeezed state, where $V(A) = \langle A^2\rangle - \langle A\rangle^2$ denotes the variance of operator A. Accordingly, by use of Eq. (5), the spectral variances and covariances of the output fields have the general form

$$\begin{aligned} S_{X_i}^{\text{out}}(\omega) &= 1 + 2\gamma_c S_{X_i}(\omega), \\ S_{X_i,X_j}^{\text{out}}(\omega) &= 2\gamma_c S_{X_i,X_j}(\omega). \end{aligned} \tag{15}$$

Similar expressions can be derived for the Y quadratures.

V. FIVE-PARTITE ENTANGLEMENT CRITERIA

The condition proposed by van Loock and Furusawa (VLF) [39], which is a generalization of the conditions for bipartite entanglement, is sufficient to demonstrate multipartite entanglement. We now demonstrate how these may be optimized for the verification of genuine five-partite entanglement in this system. Using the quadrature definitions, the five-partite inequalities, which must be simultaneously violated, are

$$\begin{aligned} S_{(1)} = {} & V(X_p + X_{s1}) + V(-Y_p + Y_{s1} + g_{i1}Y_{i1} + g_{s2}Y_{s2} \\ & + g_{i2}Y_{i2}) \geqslant 4, \end{aligned} \tag{16}$$

$$\begin{aligned} S_{(2)} = {} & V(X_p + X_{i1}) + V(-Y_p + g_{s1}Y_{s1} + Y_{i1} + g_{s2}Y_{s2} \\ & + g_{i2}Y_{i2}) \geqslant 4, \end{aligned} \tag{17}$$

$$\begin{aligned} S_{(3)} = {} & V(X_{s1} - X_{s2}) + V(g_pY_p + Y_{s1} + g_{i1}Y_{i1} + Y_{s2} \\ & + g_{i2}Y_{i2}) \geqslant 4, \end{aligned} \tag{18}$$

$$\begin{aligned} S_{(4)} = {} & V(X_{i2} - X_{i1}) + V(g_pY_p + g_{s1}Y_{s1} + Y_{i1} \\ & + g_{s2}Y_{s2} + Y_{i2}) \geqslant 4, \end{aligned} \tag{19}$$

where the $g_k(k = p,s1,s2,i1,i2)$ are arbitrary real parameters that are used to optimize the violation of these inequalities. It is important to note that, in the uncorrelated limit, these optimized VLF criterion approach four. Due to the symmetry relation between signal and idler photons, Eqs. (16) and (17) are equivalent. So are Eqs. (18) and (19). Thus, we only need to calculate $S_{(1)}$ and $S_{(3)}$.

VI. OUTPUT FLUCTUATION SPECTRA

According to Eqs. (8)–(11), the stable solution is completely determined by three parameters: the total damping rate γ, the coupling coefficient g, and the pumping power ϵ, which in turn determine the drift matrix $\boldsymbol{M}$, the diffusion matrix $\boldsymbol{D}$, and the intracavity spectral correlation matrix $\boldsymbol{S}$. Finally, the intra- and extracavity spectral correlation matrices are related by a parameter γ_c through Eq. (15). We thus conclude that these four parameters fully describe the extracavity spectral correlation. Therefore, we investigate in this section how these parameters affect the extracavity entanglement. We find that the extracavity entanglement is completely determined by three parameters: $\varepsilon/\varepsilon_{th}$, γ_c/γ, and ω/γ.

A. Effect of total damping rate

To begin with, we rewrite Eq. (8) as

$$\frac{\varepsilon}{\gamma} = \frac{\varepsilon}{\varepsilon_{th}}\sqrt{\frac{\gamma}{g}}. \tag{20}$$

By substituting Eq. (20) into Eqs. (9)–(11), we obtain

$$\begin{aligned}
\sqrt{\frac{g}{\gamma}}A_p &= \left(\frac{\varepsilon}{\varepsilon_{th}} + \sqrt{\left(\frac{\varepsilon}{\varepsilon_{th}}\right)^2 + 3}\right) \Big/ 3, \\
\sqrt{\frac{g}{\gamma}}A_a &= \sqrt{\frac{1}{4}\left(1 - \frac{\gamma}{gA_p^2}\right)}, \\
\sqrt{\frac{g}{\gamma}}A_b &= 2\left(\sqrt{\frac{g}{\gamma}}A_p\right)\left(\sqrt{\frac{g}{\gamma}}A_a\right)^2.
\end{aligned} \tag{21}$$

We find that the stable solutions $\sqrt{\frac{g}{\gamma}}A_k (k = p,a,b)$ are only determined by $\varepsilon/\varepsilon_{th}$. By using them in $\boldsymbol{D}$, $\boldsymbol{M}$, and Eq. (22), we can find

$$\boldsymbol{S}(\omega) = \frac{1}{\gamma}\left(-\frac{\boldsymbol{M}}{\gamma} + i\frac{\omega}{\gamma}\boldsymbol{I}\right)^{-1}\frac{\boldsymbol{D}}{\gamma}\left(-\frac{\boldsymbol{M}^T}{\gamma} - i\frac{\omega}{\gamma}\boldsymbol{I}\right)^{-1}. \tag{22}$$

With this result together with Eq. (15), we can see that $\boldsymbol{S}^{\text{out}}$ is completely determined by $\varepsilon/\varepsilon_{th}$, γ_c/γ, and ω/γ. Therefore, the variance $S_i(\omega/\gamma)$ (as a function of ω/γ) is solely determined by the parameters $\varepsilon/\varepsilon_{th}$ and γ_c/γ rather than by g, γ, and ε. This conclusion is verified numerically. If we decrease the values of n_2 and γ by half simultaneously while keeping $\varepsilon/\varepsilon_{th}$ constant, the noise spectrum will remain unchanged, except for a scaling factor in the frequency axis.

B. Effect of external coupling rate

From now on, we numerically calculate the values of VLF inequalities according to the results obtained above. We assume that the resonator is a spherical CaF_2 cavity. Note that the theoretical model and analysis are universal and can be easily applied to other device platforms. For CaF_2, the refractive index is $n_0 = 1.43$, the Kerr coefficient is $n_2 = 3.2 \times 10^{-20}$ m^2/W. We assume the CaF_2 resonator has a radius $R = 2.5$ mm, corresponding to an effective mode volume of $V_0 = 6.6 \times 10^{-12}$ m^3. Light is critically coupled to the device with a loaded quality factor $Q_0 = 3 \times 10^9$ (corresponding to a central modal bandwidth $\Delta\omega_0 = \gamma_p \approx 2\pi \times 64$ kHz [11]), with a pump launched at a wavelength of $\lambda_0 = 1560.5$ nm.

We first fix g, γ, and ϵ—the three parameters that determine the evolution inside the cavity—and vary the γ_c/γ ratio to see how it affects the observed entanglement. In Fig. 3, we plot the minimum of the variances versus the analysis frequency normalized to γ when γ_c takes a portion of 0.34,0.57,0.8,1 of the total damping rate. The blue dashed lines stand for $S_{(1)}$, while the green solid lines stand for $S_{(3)}$.

It can be seen from the plot that, when $\gamma_c = 0.34\gamma$, there is no entanglement between any two of the field modes. As we increase the out-coupling coefficients, the $s1$ and $i1$ begin to entangle with the pump photons around the center frequency,

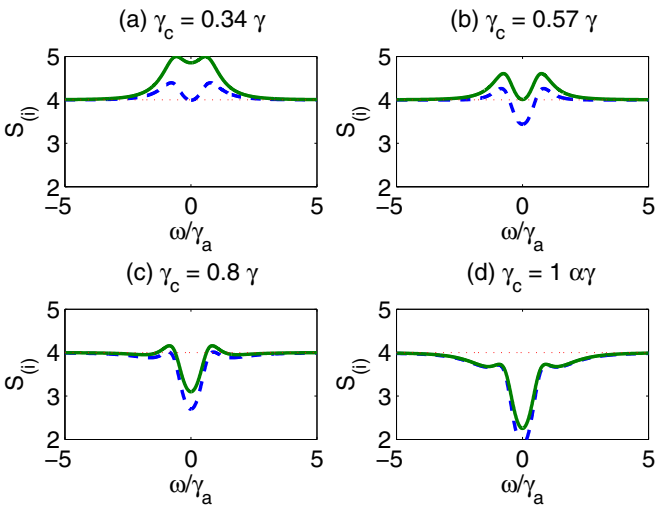

FIG. 3. (Color online) Extracavity variance versus frequency of pump plots when γ_c is 0.34,0.57,0.8,1 times as great as γ (from left to right and top to bottom). $\gamma = 4.02 \times 10^5$ s^{-1}, $g = 2.21 \times 10^{-4}$ s^{-1}, $\epsilon = 1.15\epsilon_{th} = 1.97 \times 10^{10}$ s^{-1}. The blue dashed curve stand for $S_{(1)}$ and $S_{(2)}$, whereas the green solid curves stand for $S_{(3)}$ and $S_{(4)}$. The pump power is fixed at $1.15\epsilon_{th}$.

but it is not until $\gamma_c/\gamma = 0.57$ that $s2$ and $i2$ begin to entangle with $s1$ and $i1$, respectively. Eventually the variance converges to Fig. 3(d). Thus we conclude that the entanglement among output modes is improved as the γ_c/γ ratio increases, i.e., the entanglement is better when the cavity has higher Q (and therefore lower intracavity loss) and a higher extracavity coupling coefficient. This can be interpreted naturally if we see the coupling as a beam splitter which extracts squeezed quantum noise to the output [37], so the higher portion the coupling coefficient takes in the total damping rate, the less consumed entangled pair of photons are wasted in the internal loss. For that consideration, we will ideally fix $\gamma_0 = 0$ in the following analysis, so that the effect of output transfer is suppressed to minimum.

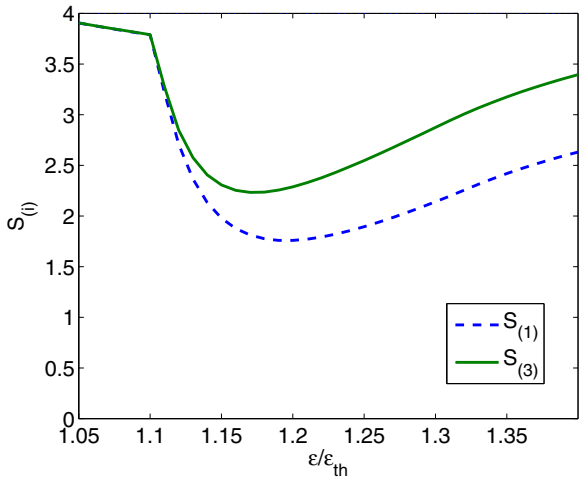

FIG. 4. (Color online) Minimum extracavity variance as a function of pump power.

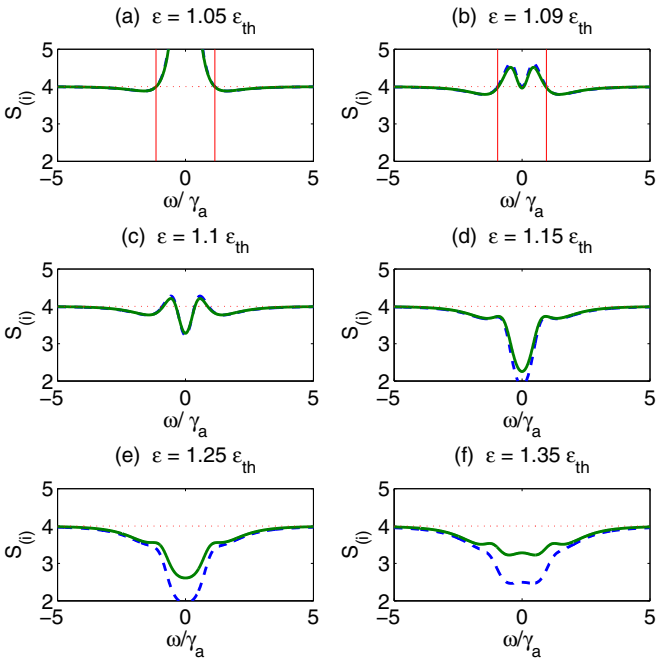

FIG. 5. (Color online) Extracavity variance versus frequency under different pumping power.

C. Effect of pump power

We plot the minimal variance throughout the noise power spectrum as a function of the pump power (normalized by ϵ_{th}) in Fig. 4 and six typical spectra in Fig. 5.

It can be inferred from the graphs that both variance first descend as the pump power increases, then ascend. $S_{(3)}$ and $S_{(4)}$ reach their global minimum at $\epsilon = 1.15\epsilon_{\text{th}}$. Considering that they are the short slabs of the whole entanglement system, we conclude that $1.15\epsilon_{\text{th}}$ is the optimal pump power. The other turning point in Fig. 4 is around $1.1\epsilon_{\text{th}}$, when, as we can see in Figs. 5(b) and 5(c), the variances in the center frequency begin to decrease dramatically and become the minimum which was once achieved in the side band, as shown in Fig. 5(a).

VII. CONCLUSIONS

In conclusion, we presented a theoretical model for the five-partite continuous-variable entanglement among five field modes based on a cascaded four-wave mixing process. By solving the Fokker–Planck equation in the P representation, we analyzed the entanglement condition when van Loock and Furusawa criteria are violated. We presented the design parameters for our experimental purpose, and they might also be utilized to build an integrated compact five-partite entanglement generator. We analytically related the threshold of pump power with cavity parameters. We found that the degree of entanglement was totally determined by ω/γ, ϵ/ϵ_{th}, and γ_c/γ. This result filled the theoretical gap for the entanglement analysis of OFCs generated from the high-Q resonator,and therefore should pave the way for future optical quantum computation on chip.

ACKNOWLEDGMENTS

This work is supported by the National Natural Science Foundation of China (Grants No. 61475099 and No. 61102053), Program of State Key Laboratory of Quantum Optics and Quantum Optics Devices (No. KF201405), the Scientific Research Foundation for the Returned Overseas Scholars, State Education Ministry, SMC Excellent Young Faculty program, SJTU 2011. Q.L. also thanks the support of National Science Foundation of the United States under Grant No. ECCS-1351697.

[1] P. W. Shor, SIAM J. Comput. **26**, 1484 (1997).
[2] R. P. Feynman, Int. J. Theor. Phys. **21**, 467 (1982).
[3] R. Raussendorf and H. J. Briegel, Phys. Rev. Lett. **86**, 5188 (2001).
[4] H. J. Briegel and R. Raussendorf, Phys. Rev. Lett. **86**, 910 (2001).
[5] N. C. Menicucci, S. T. Flammia, and O. Pfister, Phys. Rev. Lett. **101**, 130501 (2008).
[6] J. Roslund, R. Medeiros de Araújo, S. Jiang, C. Fabre, and N. Treps, Nat. Photonics **8**, 109 (2014).
[7] S. T. Cundiff and J. Ye, Rev. Mod. Phys. **75**, 325 (2003).
[8] S. A. Diddams, J. Opt. Soc. Am. B **27**, B51 (2010).
[9] P. DelHaye, A. Schliesser, O. Arcizet, T. Wilken, R. Holzwarth, and T. Kippenberg, Nature (London) **450**, 1214 (2007).
[10] T. Kippenberg, R. Holzwarth, and S. Diddams, Science **332**, 555 (2011).
[11] Y. K. Chembo and N. Yu, Phys. Rev. A **82**, 033801 (2010).
[12] D. F. Walls and G. J. Milburn, *Quantum Optics* (Springer, Berlin, 2007).
[13] R. M. Shelby, M. D. Levenson, S. H. Perlmutter, R. G. DeVoe, and D. F. Walls, Phys. Rev. Lett. **57**, 691 (1986).
[14] L.-A. Wu, H. J. Kimble, J. L. Hall, and H. Wu, Phys. Rev. Lett. **57**, 2520 (1986).
[15] L.-A. Wu, M. Xiao, and H. Kimble, J. Opt. Soc. Am. B **4**, 1465 (1987).
[16] M. Wolinsky and H. J. Carmichael, Phys. Rev. Lett. **60**, 1836 (1988).
[17] G. Breitenbach, T. Müller, S. Pereira, J.-P. Poizat, S. Schiller, and J. Mlynek, J. Opt. Soc. Am. B **12**, 2304 (1995).
[18] G. Breitenbach, S. Schiller, and J. Mlynek, Nature (London) **387**, 471 (1997).
[19] J. Laurat, L. Longchambon, C. Fabre, and T. Coudreau, Opt. Lett. **30**, 1177 (2005).
[20] H. Vahlbruch, M. Mehmet, S. Chelkowski, B. Hage, A. Franzen, N. Lastzka, S. Goßler, K. Danzmann, and R. Schnabel, Phys. Rev. Lett. **100**, 033602 (2008).
[21] H. Yonezawa, K. Nagashima, and A. Furusawa, Opt. Express **18**, 20143 (2010).
[22] Q. Lin and G. P. Agrawal, Opt. Lett. **31**, 3140 (2006).
[23] Q. Lin, O. J. Painter, and G. P. Agrawal, Opt. Express **15**, 16604 (2007).
[24] R. Osgood Jr. *et al.*, Adv. Opt. Photonics **1**, 162 (2009).

[25] J. Chen, Z. H. Levine, J. Fan, and A. L. Migdall, Opt. Express **19**, 1470 (2011).
[26] J. E. Sharping, K. F. Lee, M. A. Foster, A. C. Turner, B. S. Schmidt, M. Lipson, A. L. Gaeta, and P. Kumar, Opt. Express **14**, 12388 (2006).
[27] H. Takesue, H. Fukuda, T. Tsuchizawa, T. Watanabe, K. Yamada, Y. Tokura, and S.-i. Itabashi, *2008 Fifth IEEE International Conference on Group IV Photonics, Cardiff* (IEEE, Piscataway, NJ, 2008), pp. 404–406.
[28] H. Takesue, H. Fukuda, T. Tsuchizawa, T. Watanabe, K. Yamada, Y. Tokura, and S.-i. Itabashi, Opt. Express **16**, 5721 (2008).
[29] K.-i. Harada, H. Takesue, H. Fukuda, T. Tsuchizawa, T. Watanabe, K. Yamada, Y. Tokura, and S.-i. Itabashi, Opt. Express **16**, 20368 (2008).
[30] K.-i. Harada, H. Takesue, H. Fukuda, T. Tsuchizawa, T. Watanabe, K. Yamada, Y. Tokura, and S.-i. Itabashi, IEEE J. Sel. Top. Quantum Electron. **16**, 325 (2010).
[31] A. Coelho, F. Barbosa, K. Cassemiro, A. Villar, M. Martinelli, and P. Nussenzveig, Science **326**, 823 (2009).
[32] S. Coen and M. Erkintalo, Opt. Lett. **38**, 1790 (2013).
[33] T. Herr, V. Brasch, J. Jost, C. Wang, N. Kondratiev, M. Gorodetsky, and T. Kippenberg, Nat. Photonics **8**, 145 (2014).
[34] A. B. Matsko, A. A. Savchenkov, D. Strekalov, V. S. Ilchenko, and L. Maleki, Phys. Rev. A **71**, 033804 (2005).
[35] P. D. Drummond, in *Coherence and Quantum Optics VII* (Springer, New York, 1996), pp. 323–332.
[36] P. D. Drummond and M. Hillery, *The Quantum Theory of Nonlinear Optics* (Cambridge University Press, Cambridge, 2014).
[37] C. W. Gardiner and M. J. Collett, Phys. Rev. A **31**, 3761 (1985).
[38] C. Gardiner, *Stochastic Methods* (Springer-Verlag, Berlin–Heidelberg–New York–Tokyo, 1985).
[39] P. van Loock and A. Furusawa, Phys. Rev. A **67**, 052315 (2003).